PERFORMANCE OF A NEW EYE-SAFE 3D-LASER-RADAR APD LINE SCANNER

Bernd Eberle[(1)], Tobias Kern[(1)], Marcus Hammer[(1)], Ulrich Schwanke[(2)], Heinrich Nowak[(2)]

[(1)]Fraunhofer Institute of Optronics, System Technologies and Image Exploitation IOSB, Gutleuthausstrasse 1, 76275 Ettlingen, Germany, Email: bernd.eberle@iosb.fraunhofer.de

[(2)]EADS Deutschland GmbH CASSIDIAN, Claude-Dornier-Strasse 1, 88090 Immenstaad/Bodensee, Germany, Email: heinrich.nowak@cassidian.com

KEYWORDS:
3D imaging, laser radar, active imaging

ABSTRACT:

This paper presents first results of the performance of a recently developed 3D imaging laser radar sensor, working in the short wave infrared (SWIR) at 1.5 µm. It consists of a novel Cadmium Mercury Telluride (CMT) linear detector array with 384x1 APD elements at a pitch of 25 µm, developed by AIM Infrarot Module GmbH. The APD elements were designed to work in the linear (non-Geiger) mode. Each pixel is capable to provide time of flight measurement, and, due to the linear detection mode, allowing the detection of three successive echoes. We discuss various sensor concepts regarding possible applications and their dependence on system parameters like field of view, frame rate, spatial resolution and range of operation.

1. INTRODUCTION

In a non-cooperative environment, imaging 3D laser radar sensors offer a unique potential compared to passive sensors regarding tasks like surveillance, detection of small objects, reconnaissance, classification, protection, obstacle avoidance, positioning, terrain modelling, depth sounding, autonomous navigation, automatic object recognition as well as object tracking.

Their outstanding performance is owed to the fact that laser range depth resolution is independent from the sensor's distance to the target. Specific sensor concepts with depth resolutions from tens of centimetres down to millimetres are available, see for example [1].

Today, the civil market provides quite a number of different 3D-Sensors covering ranges up to 1 km. However, the majority of imaging laser radar systems developed so far is based on two-dimensional mechanical scanning [2, 3] of the laser beam over the scene. The 3D image is built up by a series of successive laser pulses. Each return-pulse will deliver range, calculated from the time interval between emitting and receiving the laser pulse, and ideally also intensity information. Some systems are designed to capture the full waveform of the received laser pulse and will be used for sophisticated data processing purposes to analyse in addition also object specific structures.

Beside systems operating with short, typically nanosecond laser pulses at a wavelength of 1.5 µm, there are also well established systems, particularly for short range missions. They are based on frequency modulated continuous wave (FMCW) laser radiation whereby the range information is related to the phase-shift between transmitter and receiver signals [4]. A third kind of concepts uses quasi-continuous wave laser radiation, with pulse repetition rates in the range of Megahertz [5]. The latter two concepts will not be discussed further in this paper.

Employing scanning laser systems the proof was made that laser radar sensors offer the capability of automatic data evaluation [6, 7, 8]. In contrast to passive sensors where reliable object recognition algorithms are missing the main difficulty in introducing operational laser radar systems is owed to the lack of adequate sensors.

Two-dimensional scanning systems suffer from the drawback of spatial resolution, when for a given field of view (FOV) a high image update rate is necessary.

Tasks demanding reliable resolution of small objects, especially at long ranges in real time can be fulfilled only by sensors consisting of detector arrays. The detector has to be seen as the heart of an imaging 3D sensor system that ensures suffi-

cient frame rates and high spatial resolution for tasks like detection or classification [9, 10, 11].

Increasing efforts were made worldwide to develop 3D-detectors based on one- or two-dimensional arrays. The detector developments concentrate on avalanche photo detectors (APD) operated in the Geiger mode (GAPD) or in the linear (non-Geiger) mode. GAPDs offer the advantage of higher sensitivity, but there are also some negative effects using GAPDs in laser radar: First, dark counts generated by thermal noise can cause false alarms. Second, GAPDs experience a dead time in which the detector element does not work after detecting a photon. The dead time typically varies from 10 ns to 1 µs and depends on the detector material and on the design of the quenching electronics. Thus usually only one echo may be detected in the Geiger mode. In the linear mode multiple successive echoes can be detected within a short range.

One- and two-dimensional detector arrays are manufactured by various companies. For example Mitsubishi [12] developed a linear detector array with 256 detector elements based on InAlAs working at 1.06 µm, and Advanced Scientific Research (ASC, [13, 14]) developed a detector array of 128x128 elements working at 1.57 µm.

A different sensor technology is based on gateable two-dimensional detector arrays to be used for gated- or tomoscopic-viewing. Intevac [15] developed a SWIR camera based on Electron Bombarded Active Pixel Sensor (EBAPS®) technology. Selex [16] and CEA-Leti [17] developed 3D APD Focal Plane Arrays to be used in passive or active modes. The depth resolution for a single laser pulse depends on the width of the laser pulse and on the time the gate of the camera is open. Applying a series of laser pulses in conjunction with a sliding gating technique, the depth resolution can be improved to values of about 30 cm.

2 SYSTEM DETAILS

The investigated 3D laser range camera consists of a novel linear detector array with 384x1 Avalanche Photo Diode (APD) elements at a pitch of 25 µm, developed by AIM Infrarot Module GmbH, Germany. As detector material Cadmium Mercury Telluride (CMT) was chosen. The APD elements operate in the linear mode to allow the required detection of three successive echoes, which is not possible in the Geiger mode as explained above.

The digital read out integrated circuit (ROIC) was designed to offer a principal depth resolution of 60 cm. Using additional electronic processing on the ROIC a depth resolution of 15 cm could be attained. The ROIC delivers the time-of-flight (TOF) data for the flashed area at once and for test purposes an intensity mode is offered. The maximum read-out rate is 4 kHz.

Besides the 3D-detector an imaging-laser-radar requires a suitable transmitter and receiver optics, a sufficient powerful laser source and a scan-unit. Moreover, setting-up a scanning laser-radar system requires adequate system parameters like laser pulse energy, pulse repetition rate, field of view, 3D-camera frame rate, and an adapted resolution for scanner and optics as well. All the before mentioned parameters are governed by the task-specific boundary conditions.

Let's consider a simple example to illustrate the correlation between the various parameters: Tasks like ATR on long ranges (> 1 km) or collision avoidance on short ranges (< 200 m) will lead to diverging FOVs. In turn on that the FOV determines the necessary focal length of the receiver lens which again influences the effective lens aperture. The lens aperture, together with the laser output power, rules the received power on the detector. Again in turn, depending on the sensor's sensitivity, the considered task may be accomplished or not. If not, we have to redesign the system.

Trying to realize a FOV of around five degree, just for the present test purposes, we chose a commercial SWIR lens from Optec S.p.A. with an f-number of 100/1.4 as receiver optics for the 3D laser range camera. To suppress background radiation, a bandpass filter of 80 nm width was mounted in the back of that lens.

The other crucial part in an imaging 3D laser range system is the transmitter. Due to a lack of a kHz-laser system we used a Q-switched 20 Hz OPO laser from Quantel (Big Sky CFR 400 Laser Series) with an output power of 70 mJ at the wavelength of 1.57 µm.

The transmitter optics, developed by EADS-Deutschland GmbH Cassidian, was designed to fit the linear FOV of the receiver. It consists of three lenses (Fig. 1) whereby the second lens is a cylindric one. The intensity profile of the long axis of the laser beam is shown, as simulated, in Fig. 2. The cross section of the laser line was measured in the field at a distance of 112 m (see Fig. 3). It turned out that the line width was 1.5 mrad as expected by the optical simulation of the lens.

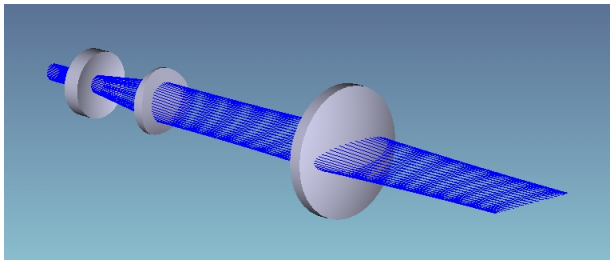

Figure 1. Laser transmitter optics, designed to form a laser beam with a linear shape. In the far field, the laser line turns to the vertical orientation.

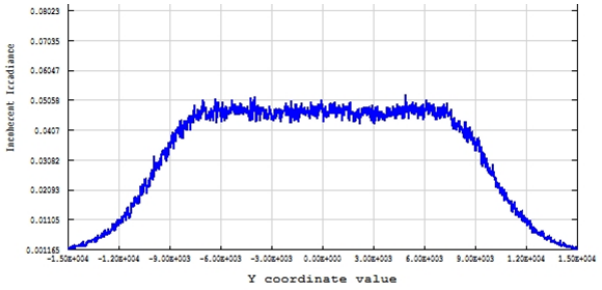

Figure 2. Laser-line-profile along the length-axis at a simulated distance of 200 m.

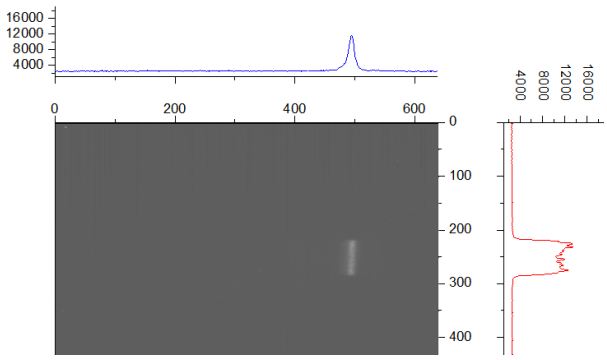

Figure 3. Laser-line-width profile on a 1 m high retro-reflecting target at a distance of 112 m, viewed with a SWIR-camera.

The sensor head, consisting of the 3D-camera and the laser source (see Fig. 4), but also of a SWIR-camera to monitor the laser beam, were mounted on a horizontally scanning rotation stage. This scan direction was attributed to the fact, that the 3D-camera was mounted with the detector line in the vertically direction.

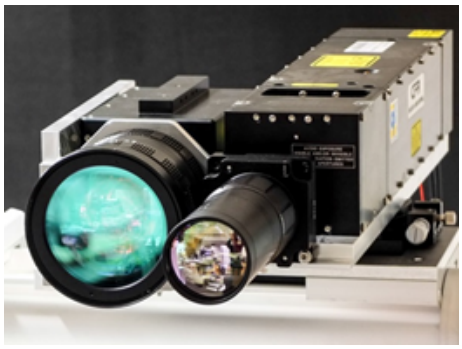

Figure 4. View of the 3D line-detector camera (left) and the laser source (right) equipped with lenses.

The whole experimental set-up was operated by a home-build computer control. It ensured all triggering of the 3D-camera, the laser and the scanning unit, as well as data recording and real-time visualization of the measured range data. A sketch of the measurement system is shown in Fig. 5.

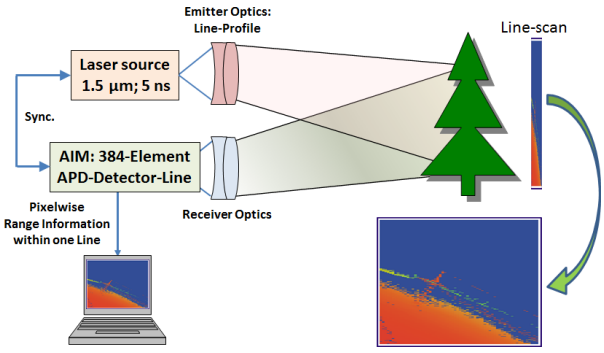

Figure 5. Sketch of the measurement system to illustrate the data acquisition principle.

3. RESULTS

The 3D laser radar system was set-up in a laboratory from which the surrounding environment could be accessed. A visual impression of the scene is shown in Fig. 6. In a first step the laser line and the sensor's FOV had to be overlayed to each other. For this purpose the laser was targeted to an exterior wall of a building close to the laboratory on the right hand side (not visible).

With the help of a SWIR camera the position and the orientation of the laser line could be monitored. Using the intensity mode of the 3D-range camera the laser beam was adjusted horizontally and vertically to create homogenous signal levels along the detector line.

Figure 6. Visual impression of the environmental surrounding of the laboratory. The range to the high building on the left hand side of the scene is 270 m.

During data acquisition each of the three echoes was visualized in real-time on the monitor of the control computer. That is, the raw data for each single laser shot were successively plotted line for line to compose the range images.

Fig. 7 and Fig. 8 show raw data range images for the first and the second echo, respectively, with a size of 384x600 pixels. The horizontal step width was adjusted to the vertical pixel spacing corresponding to an instantaneous field of view (IFOV) of 5°FOV / 384 detector elements.

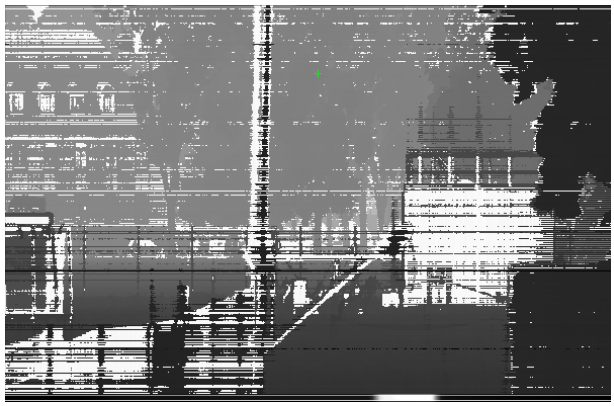

Figure 7. Range image of the 1st echo of the scene, based on unprocessed range data, represented in grey scales.

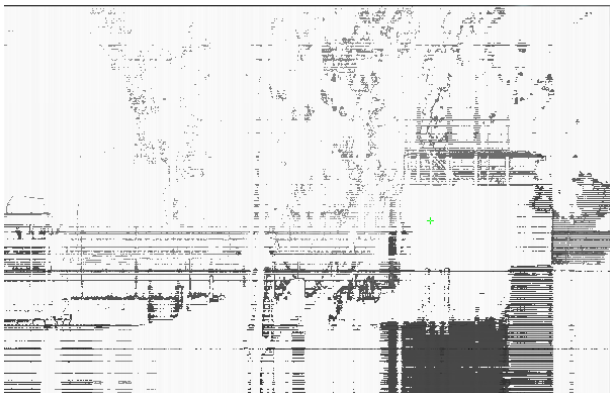

Figure 8. Range image of the 2nd echo of the scene, based on unprocessed range data, represented in grey scales.

It is remarkable that in the first echo the grass field and the trees are represented by homogenous areas. In contrast to that, the house in the background (wall, roof), the two white coloured containers, the metal fence in the foreground left and the pole in the middle of the scene, show varying range data. That is mainly owed to the fact of saturation effects which lead to invalid range data or, in the case of the roof, to returns of too small signals.

Fig. 9 and Fig. 10 show processed range images for the first echo represented in false colours and in grey scales, respectively. The main difference to the raw (unprocessed) range data in Fig. 7 and Fig. 8 is that data with invalid ranges (i.e. signal

overflow) were filtered out. As a result, many of the white stripes were eliminated. Now, in both representations (false colours and grey scales) the depth information is clearly recognizable.

Significant changes in the range images may be observed at the two (in the visible) white coloured containers. The unprocessed range data of these containers, presented in grey scales, also appear in white, since most of the laser returns create a signal overflow (end of range information). Due to data processing the remaining pixels show the correct range value or they were set to zero.

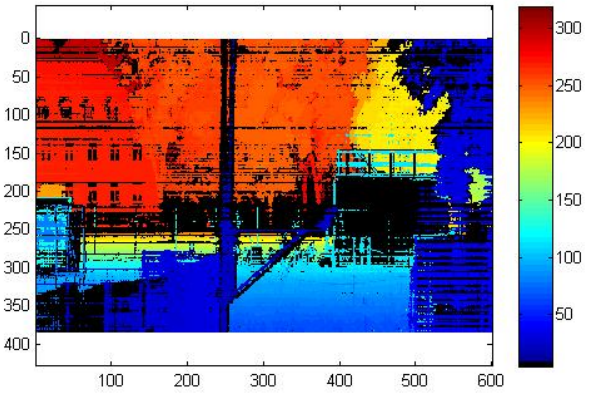

Figure 9. Depth image of the measured scene composed of processed data, coded in false colours.

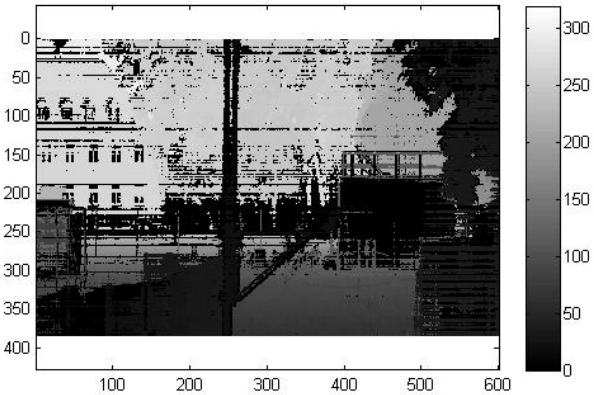

Figure 10. Depth image of the measured scene composed of processed data, coded in grey scale.

To estimate the performance of the scanning laser radar, it was compared with a staring one: The "Portable 3D Flash LIDAR Camera" from Advanced Scientific Concepts Inc. It consists of a detector array of 128x128 elements together with a 12 mJ laser emitting at a wavelength of 1.5 µm. The heart of the system is a multifunction ROIC based upon both analog and digital processing. The integrated circuit of each detector element outputs a pulse profile of the reflected signal. The range for each pixel is calculated by finding the maximum of a smooth curve fitting the digitized pulse. This achieves a sub-sampling range accuracy of about 15-20 cm.

The location of the ASC-Sensor was about 8 m away from the line scanning camera, so the positions of various characteristic elements in the scene appear at different positions. Fig. 11 shows a range image, when the sensor was equipped with an FOV = 9° optics.

The white pixels result from low signal levels, since the 12 mJ laser energy was distributed over the full field of view. Moreover, the pixel density of the ASC-sensor on the targets is much lower compared to the line-scanning system, and results, in one direction, in a factor of about five between the two systems. Thus the building in the distant part of the scene looks "less good" compared to the scanned images in Fig. 9 or Fig. 10.

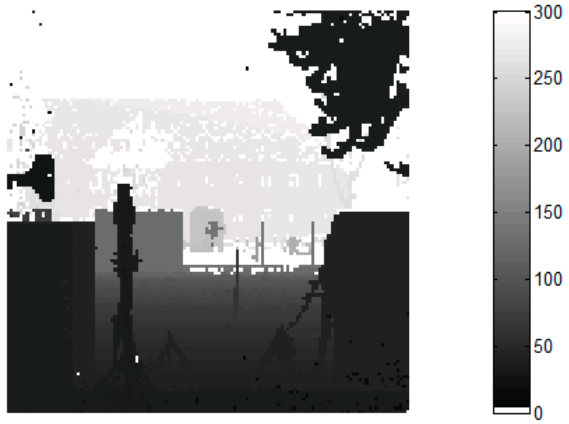

Figure 11. For comparison: ASC-LADAR sensor image, taken from a slightly different measurement position compared to the SFL-sensor.

The depth resolution was estimated by analyzing a single line pointed at the wall of the house at a distance of 270 m. It turned out that the ASC sensor nearly reaches its theoretical resolution of about 20 cm. Due to problems in the electronics/firmware of the 3D-line camera only the basic resolution range data could be accessed. Thus the resulting error in depth was around two times the basic resolution. After checking the causes of these problems the sensor performance will be investigated in more detail.

5. SUMMARY

We reported on first results of a recently developed scanning SWIR 3D imaging laser radar sensor working at 1.5 µm. The detector consists of a linear array of 384x1 APD elements based on Cadmium Mercury Telluride (CMT) and designed to work in the linear (non-Geiger) mode.

We could prove that the sensor delivers three echoes with complementary information. Although the sensitivity of the single APD elements across the detector line exhibited some inhomogeneities the quality of the resulting range data was admirable.

In a next step the range resolution will be improved by implementing a new firmware and then the sensor's performance will be analyzed in more detail.

6. REFERENCES

1. http://www.gim-international.com/issues/articles/id1629-Terrestrial_Laser_Scanning.html
2. Schulz, K., Scherbarth, S., Fabry, U. (2002). Hellas: Obstacle warning system for helicopters. *Proc. SPIE* **4723**, p. 1–8.
3. http://www.riegl.com/
4. http://www.zf-laser.com/Home.91.0.html
5. McCarthy, A. et al. (2013). Kilometer-range, high resolution depth imaging via 1560 nm wavelength single-photon detection. *Opt. Express* **21**(7), p. 8904–8915.
6. Bers, K., Schulz, K., Armbruster, W. (2005). Laser radar system for obstacle avoidance. *Proc. SPIE* **5958**, p. 59581J-1.
7. Armbruster, W. (2009). Exploiting range imagery: techniques and applications. *Proc. SPIE* **7382**, p. 738203-1.
8. Steinvall, O. et al. (2004). 3-D laser sensing at FOI – overview and a system perspective. *Proc. SPIE* **5412**, p. 294–309.
9. Grönwall, C. et al. (2010). Threat Detection and Tracking using 3D FLASH LADAR Data. *Proc. SPIE* **7696**, p. 76960N-1.
10. Armbruster, W., Hammer, M. (2010). Maritime target identification in flash-ladar imagery. *Proc. SPIE* **8391**, p. 83910C-1.
11. Armbruster, W., Hammer, M. (2012). Segmentation, classification, and pose estimation of maritime targets in flash-ladar imagery. *Proc. SPIE* **8542**, p. 85420K-1.
12. Kameyama, S. et al. (2011). Development of long range, real-time, and high resolution 3-D Imaging LADAR. *Proc. SPIE* **8192**, p.819205-1
13. http://advancedscientificconcepts.com/
14. Stettner, R. (2010). Compact 3D Flash LIDAR video cameras and applications. *Proc. SPIE* **7684**, p. 768405-1.
15. http://www.intevac.com/intevacphotonics/vision-systems/vision-systems-products/livar-506/
16. Baker, I. et al. (2012). Developments in MOVPE HgCdTe Arrays for Passive and Active Infrared Imaging. *Proc. SPIE* **8542**, p. 85421A-1.
17. De Borniol, E. et al. (2012). Active three-dimensional and thermal imaging with a 30-µm pitch 320 × 256 HgCdTe avalanche photodiode focal plane array. *Opt. Eng.* **51**, p. 061305-1.